Surface polariton generation and fluorescence enhancement using a superlens

Yingjie Zhang, Ruoyang Zhang, Zhishuai Zhang, Haibo Zhu, and Feng Song*

Photonics Center, School of Physics, Nankai University, Tianjin 300071, China
**Corresponding author: fsong@nankai.edu.cn*

Received September 8, 2009; revised October 20, 2009; accepted October 22, 2009;
posted October 22, 2009 (Doc. ID 116805); published November 17, 2009

We present a theoretical study of fluorescence enhancement in the vicinity of a superlens slab, the other side of which is connected to a prism. The fluorescent molecule is regarded as an electric dipole. The dipole excitation rate follows Fermi's golden rule, while its relaxation process has several pathways that can be analyzed within the range of classical electromagnetic theory. The calculated results are explained by surface modes and reveal a great potential of the proposed configuration in enhancing and detecting fluorescence. © 2009 Optical Society of America

OCIS codes: 160.3918, 220.0220, 240.5420, 260.2510.

1. INTRODUCTION

It is known that the fluorescence processes of quantum emitters are influenced by their surrounding environment, especially metallic structures. Specifically, fluorescence processes near thin metal films with a width of less than 50 nm have been studied extensively, and the role of surface plasmons on fluorescence excitation and emission processes has been demonstrated [1–8]. Surface plasmons can be generated when the parallel component of the wave vector of the incident plane wave matches the surface plasmon wave vector. The exciting properties of surface plasmons result from the fact that the dielectric permittivity of the metal is negative, while its magnetic permeability is the same as that of the vacuum. Hence, it is intriguing to go one step further and study the surface modes of the material with both negative dielectric permittivity and magnetic permeability, together with their influence on fluorescence. This kind of material is called a left-handed material (LHM), which was predicted by Veselago [9] and was experimentally demonstrated by Smith *et al.* in the centimeter wave range [10]. The most peculiar kind of LHM is the superlens pointed out by Pendry [11], a material with both $\varepsilon(\omega)=-1$ and $\mu(\omega)=-1$ at a specific frequency.

The surface modes of a LHM are called surface polaritons (SPs) and have been widely studied recently [12–15]. These studies focus mainly on the SP dispersion relations. As to the superlens, theoretical studies show that it can influence the fluorescent relaxation rates of nearby molecules [16–18]. To the best of our knowledge, there has been no study addressing both the excitation and relaxation processes of fluorescent molecules in the vicinity of LHMs.

In this paper, we propose a new configuration involving a prism and a superlens, which can be used to excite a SP and enhance molecular fluorescence and improve its detection efficiency. The fluorescence process is divided into two independent steps: excitation and relaxation. In both processes, the fluorescent molecule is approximated as an electric dipole. Semiclassical analysis is adopted to explain the excitation enhancement mechanism, while a full classical approach is taken to calculate the excitation enhancement factor and analyze the relaxation process. Calculated analytical results are explained by SP modes throughout this paper.

2. CONFIGURATION

Since SPs are characterized by evanescent fields, they cannot be excited directly by an electromagnetic plane wave. To generate SPs in the interface between LHMs and right-handed materials (RHMs), the attenuated total reflection technique is widely used [12,13,15], which is illustrated in Fig. 1. In [12,13,15], polariton dispersion relations are deduced by assuming the proper form of surface modes that satisfy Maxwell's equations and subsequently applying the boundary conditions . The reflectivity of the attenuated total reflection configuration as a function of the incident frequency is also calculated, and the dips in the reflectivity curve prove the existence of SPs.

In this paper, our interest lies in enhancing fluorescence by generating a SP, which is characterized by a highly localized field with strong intensity. To realize this goal, a new configuration with a prism and a superlens is proposed, as is shown in Fig. 2. There are mainly two differences of this configuration as compared with the one illustrated in Fig. 1. First, the gap between the prism and the LHM is reduced to zero. Second, the LHM layer is assumed to be a superlens, whose dielectric permittivity and magnetic permeability have a real part of −1 in the fluorescence excitation frequency ω_0. These two choices are made in order to achieve maximum field intensity in the lower surface of the LHM. Specifically, if there is a large vacuum gap between the prism and the LHM, the field will decay exponentially in the gap, resulting in a

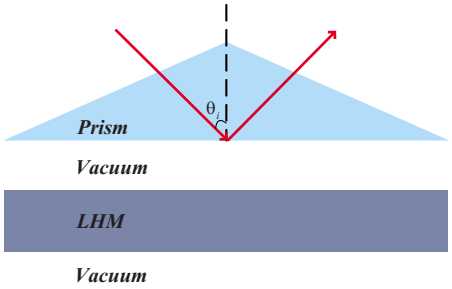

Fig. 1. (Color online) One widely used configuration used to excite SPs in the two vacuum–LHM interfaces. θ_i denotes the incident angle of the plane wave.

low coupling efficiency between the incident wave and the SP mode. When the vacuum gap is small, the field enhancement in the lower surface of the LHM should be approximately the same as the case when the gap disappears. These two conclusions are validated by our calculated results (not shown here). Therefore, we reduce the gap width to zero so as to achieve maximum field enhancement in the lower surface of the LHM. Meanwhile, this also makes the configuration simpler. In this case, when a plane wave is incident on the LHM through the prism, a SP cannot be generated in the prism–LHM interface. However, a SP mode can exist in the LHM–vacuum interface if the following relation is satisfied [12,15]:

$$\frac{\beta_2}{\mu_2(\omega)} + \frac{\beta_3}{\mu_3} = 0 \quad \text{for } s \text{ polarization}, \tag{1}$$

$$\frac{\beta_2}{\varepsilon_2(\omega)} + \frac{\beta_3}{\varepsilon_3} = 0 \quad \text{for } p \text{ polarization}, \tag{2}$$

where

$$\beta_j = (k_x^2 - \varepsilon_j \mu_j \omega^2/c^2)^{1/2}, \quad j = 1,2,3. \tag{3}$$

Here $k_x = \sqrt{\varepsilon_1\mu_1}\omega/c \sin\theta_i$ is the wave vector component in the x axis (which is the same in the three media), while β_j is related to the wave vector component in the z axis $k_{z,j}$ by $\beta_j = -ik_{z,j}$; ε_j and μ_j are the dielectric permittivity and magnetic permeability of the medium j (shown in Fig. 2).

For s polarization, the amplitude of the electric field can be expressed as

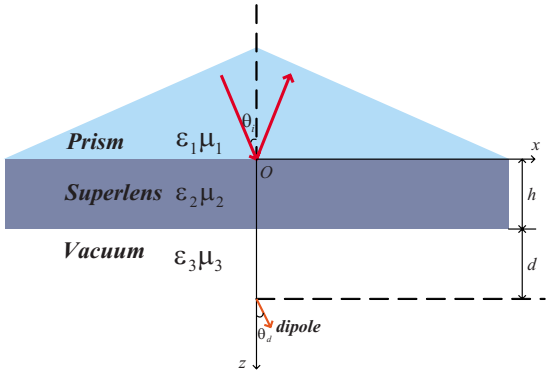

Fig. 2. (Color online) Proposed configuration to excite SP and enhance fluorescence. The fluorescent molecule is regarded as a dipole, the orientation of which has a separation angle of θ_d with the z axis.

$$\mathbf{E} = \hat{e}_y A \exp[\beta_2(z-h) + ik_x x], \quad 0 < z < h,$$

$$\mathbf{E} = \hat{e}_y B \exp[-\beta_3(z-h) + ik_x x], \quad z > h, \tag{4}$$

where $\hat{e}_y$ is the unit vector in the y direction, A and B are coefficients determined by boundary conditions, and h is the width of the superlens (shown in Fig. 2). For vacuum, $\varepsilon_3 = \mu_3 = 1$. If we set $\varepsilon_2(\omega_0) = \mu_2(\omega_0) = -1$, the LHM becomes a superlens at the fluorescence excitation frequency ω_0. According to Eq. (3), we can obtain the relation $\beta_2(\omega_0) = \beta_3(\omega_0)$. Thus Eqs. (1) and (2) are satisfied at the frequency ω_0. Therefore, a SP is generated in the superlens–vacuum interface at this frequency as long as the condition $\beta_j > 0$ is satisfied (so that the wave decays exponentially with the distance from the surface).

To test the effectiveness of this configuration to excite a SP, we calculate the reflectivity of the superlens as a function of the incident angle. In all of the following calculations, the incident field is chosen to be s polarized (the case of p polarization was also calculated, and similar results were obtained, which are not shown here). Various parameters in the numerical simulation are taken as follows: $\varepsilon_1 = 2.2$, $\mu_1 = 1$, $\varepsilon_3 = \mu_3 = 1$. The width of the superlens is chosen as $h = \lambda_0$, where $\lambda_0 = 2\pi c/\omega_0$ is the wavelength of the incident plane wave corresponding to the excitation frequency of the fluorescent molecule. As to $\varepsilon_2(\omega_0)$ and $\mu_2(\omega_0)$, four instances are considered, corresponding to different imaginary parts of the two parameters (shown in Fig. 3). Electromagnetic fields are calculated by a transfer matrix algorithm [19]. The results for the reflectivity are shown in Fig. 3. In all four cases, the reflectivity is very small below the critical angle $\theta_c = \arcsin(1/\sqrt{\varepsilon_1\mu_1}) = 42.4°$. Above this angle, total internal reflection occurs on the prism–superlens interface, and the four curves begin to separate. When $\mathrm{Im}(\varepsilon_2) = \mathrm{Im}(\mu_2) = 0$, the reflectivity remains unity above the critical angle, since there is no absorption of energy in this case. However, this does not necessarily mean a SP is not generated. In fact, the SP mode is highly localized with strong intensity in this perfect condition, revealed in the following paragraphs [see Figs. 4(d) and 5(d)]. When $\mathrm{Im}(\varepsilon_2) = \mathrm{Im}(\mu_2) \neq 0$, the existence of a SP will inevitably result in a dip in the reflectivity curve, since the propagation of the SP leads to energy absorption in this case. These dips are clearly revealed in Fig. 3; they shift left and become narrower with the increase in $\mathrm{Im}(\varepsilon_2)$ and $\mathrm{Im}(\mu_2)$.

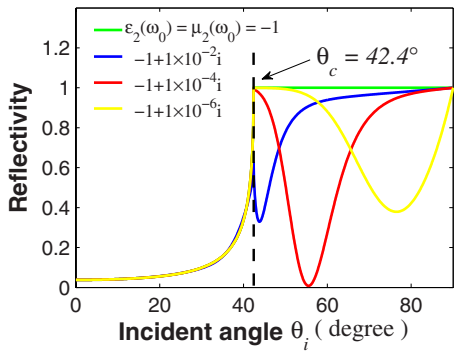

Fig. 3. (Color online) Reflectivity of the superlens. The bottom positions of the dip (from left to right) are 43.8°, 55.5°, and 76.5°, respectively.

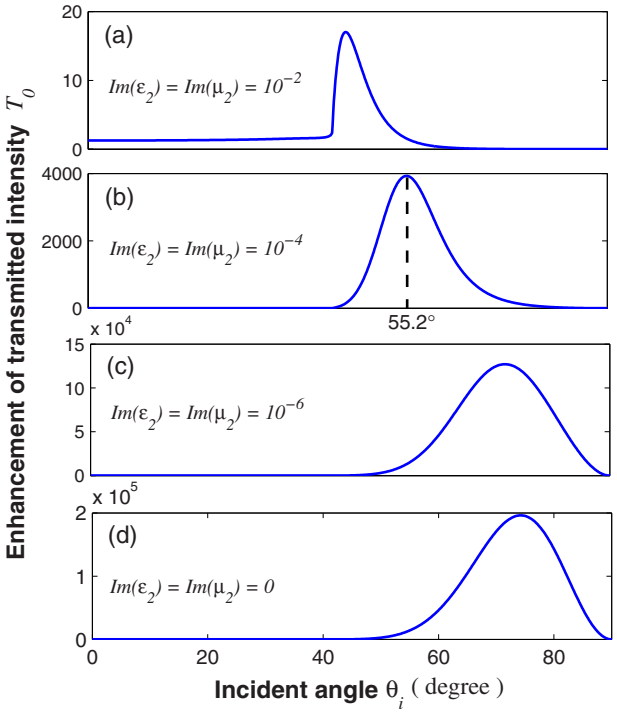

Fig. 4. (Color online) T_0 versus incident angle. The peak positions in (a), (b), (c), and (d) are 44.7°, 55.2°, 71.8°, and 74.2°, respectively.

We have also calculated the enhancement factor of the transmitted intensity (i.e., enhancement of $|\mathbf{E}|^2$ at the superlens–vacuum interface), denoted T_0. The results are presented in Fig. 4. We can see that the peak value of T_0 increases dramatically with the decrease in $\mathrm{Im}(\varepsilon_2)$ and $\mathrm{Im}(\mu_2)$. This is because the coupling between the incident wave and the SP mode becomes stronger when $\mathrm{Im}(\varepsilon_2)$ and $\mathrm{Im}(\mu_2)$ decrease. When $\mathrm{Im}(\varepsilon_2)=\mathrm{Im}(\mu_2)=0$, Eq. (1) is perfectly satisfied, and the incident wave is totally coupled to the SP mode.

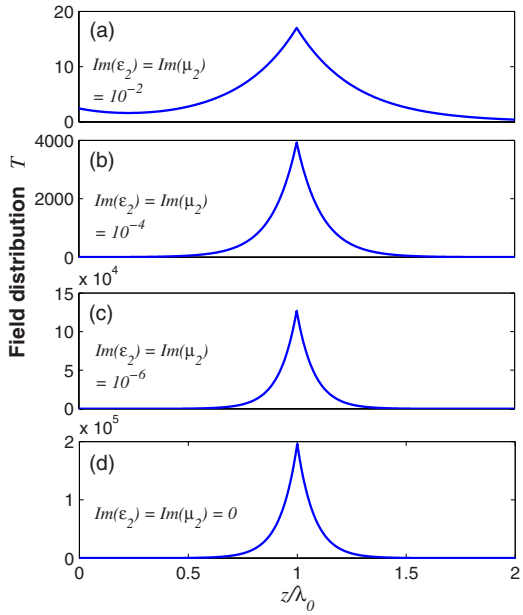

Fig. 5. (Color online) Field distribution T versus z/λ_0. The incident angles in (a), (b), (c), and (d) are chosen as the peak positions in Fig. 4(a), (b), (c), and (d), respectively. For (b), (c), and (d), the field pattern of exponential decay on both sides of the superlens–vacuum interface is observed, clearly indicating the existence of SP modes.

To further reveal the properties of the SP modes, we calculate the field distribution T (enhancement of $|\mathbf{E}|^2$) in the superlens and the vacuum. Results are shown in Fig. 5. It can be seen that the field is more confined to the surface when $\mathrm{Im}(\varepsilon_2)$ and $\mathrm{Im}(\mu_2)$ become smaller. This result can be well explained by previous conclusions. In fact, according to Fig. 3, a larger θ_i is needed to excite SPs when $\mathrm{Im}(\varepsilon_2)$ and $\mathrm{Im}(\mu_2)$ become smaller. A larger θ_i results in a larger k_x and larger β_2, β_3 [See Eq. (3)]. From Eq. (4), we can see that the SP wave is confined in the distance range $1/\beta_2+1/\beta_3$, which is reduced with the increase in β_2 and β_3. Therefore, the decrease in $\mathrm{Im}(\varepsilon_2)$ and $\mathrm{Im}(\mu_2)$ leads to greater confinement of the SP mode.

3. EXCITATION ENHANCEMENT

In this section, we briefly deduce the fluorescence excitation enhancement corresponding to the proposed configuration illustrated in Fig. 2. For the fluorescent emitter, we adopt the dipole approximation method and write its Hamiltonian as $-\mathbf{p}\cdot\mathbf{E}$, where $\mathbf{p}$ is the dipole moment and $\mathbf{E}$ is the local electric field at the position of the dipole. According to Fermi's golden rule, the probability that the emitter is excited is proportional to the square of the modulus of the perturbation Hamiltonian. Thus, the enhancement factor for fluorescence excitation can be expressed as

$$h_{\mathrm{ex}}(\omega_0) = \frac{|\mathbf{p}\cdot\mathbf{E}_d'|^2}{|\mathbf{p}\cdot\mathbf{E}_d|^2}, \tag{5}$$

where $\mathbf{E}_d'$ and $\mathbf{E}_d$ denote the electric field at the dipole point with and without the prism and superlens, respectively. Further assuming that the dipole corresponding to the excitation process is oriented randomly, we can write the excitation enhancement factor as follows:

$$h_{\mathrm{ex}}(\omega_0) = \frac{|\mathbf{E}_d'|^2}{|\mathbf{E}_d|^2}. \tag{6}$$

Therefore, the excitation enhancement is equal to the field enhancement T in the vacuum side, corresponding to the results in Fig. 5 for $z>\lambda_0$.

4. EMISSION ENHANCEMENT

In the relaxation process, the fluorescent molecule is regarded as a classical dipole. In order to analyze the influence of the prism and superlens on the fluorescence relaxation process, we will briefly reintroduce several basic concepts introduced in [20]. As is depicted, the total rate of energy dissipation for a dipole in the vicinity of the layered medium is divided into three parts:

$$P_{\mathrm{total}} = P_r + P_m + P_i, \tag{7}$$

where P_r is the radiated power, P_m is the radiation dissipated in the superlens, and P_i is the intrinsically dissipated power, which is independent of the surrounding en-

vironment of the dipole. The radiated power can be further divided into two parts:

$$P_r = P^{\uparrow} + P^{\downarrow}, \tag{8}$$

where $P^{\uparrow}$ and $P^{\downarrow}$ are the power radiated into the upper half-space and lower half-space, respectively. $P^{\uparrow}$ consists of two parts:

$$P^{\uparrow} = P_a^{\uparrow} + P_f^{\uparrow}. \tag{9}$$

Here $P_a^{\uparrow}$ is the power radiated into the allowed zone, corresponding to the Poynting vector with the direction in the range of the critical angle θ_c. $P_f^{\uparrow}$ is the power radiated into the forbidden zone, with the direction of the Poynting vector beyond θ_c.

The quantum efficiency of the dipole is defined as the fraction of the radiated power to the total dissipated power. If we write the total dissipated power and the quantum efficiency of the isolated dipole as P_0 and q_i, and write the quantum efficiency of the dipole in the vicinity of the superlens as $q = P_r/P_{\text{total}}$, then the enhancement factor of the quantum efficiency can be written as

$$h_q = \frac{q}{q_i}. \tag{10}$$

Considering that we may detect only part of the released radiation, we introduce the apparent quantum efficiency $q^{\uparrow} = P^{\uparrow}/P_{\text{total}}$ and $q^{\downarrow} = P^{\downarrow}/P_{\text{total}}$ as the ratio of detected power in the upper half-space and that in the lower half-space to the total dissipated power, respectively. And the apparent enhancement factors are $h_q^{\uparrow} = q^{\uparrow}/q_i$ and $h_q^{\downarrow} = q^{\downarrow}/q_i$, respectively.

The above physical values are calculated by using the method of angular spectrum representation provided in [20], in which the dipole field is decomposed into plane waves and evanescent waves with different wave vectors, and the transmitted field of each component is calculated before they are added together. The emission wavelength is assumed to be the same as the excitation wavelength, and the permittivity and permeability of the superlens are taken to be $\varepsilon_2(\omega_0) = \mu_2(\omega_0) = -1 + 1 \times 10^{-4} i$. The results are shown in Fig. 6. In this paper we only show the results for the dipole oriented perpendicular to the surface of the superlens ($\theta_d = 0$). In the case of parallel orientation, our calculation reveals similar results (not shown here). The interest in this paper lies in the region where the dipole–superlens distance d is very small ($d < \lambda_0$), since this is where the fluorescent molecule experiences great excitation enhancement [see Fig. 5(b)]. We can see from Fig. 6 that in this region the radiative decay rate is greatly enhanced, and that most of the radiated power goes into the forbidden zone in the upper half-space. This can be explained by the surface polariton-coupled emission algorithm, similar to the surface plasmon-coupled emission in the case when the superlens is replaced with a thin metal slab [1–8].

To analyze the surface polariton-coupled emission process in detail, the radiation pattern (defined as $p(\theta, \varphi)/P_0$, where $p(\theta, \varphi)$ is the radiated power per unit solid angle) of the dipole is calculated by using the expression provided in [20]. The results are shown in Fig. 7. We can see that most of the radiation goes into the forbidden zone in the

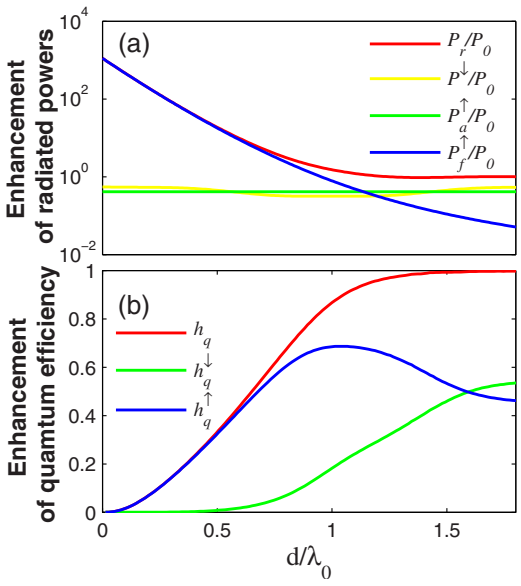

Fig. 6. (Color online) (a) Enhancement of various radiated powers versus the distance of the dipole from the lower surface of the superlens. We can see that $P_f^{\uparrow}$ is the dominant part of P_r when $d < \lambda_0$. (b) Enhancement of quantum efficiency.

upper half-space ($90° < \theta < 180° - \theta_c$) and that the peak point of the radiation pattern lies near $180° - 55.2° = 124.8°$ when d is small enough. Note that 55.2° is exactly the incident angle corresponding to the peak position of the excitation enhancement factor [see Fig. 4(b)]. Besides, according to Eq. (3) and the condition $\beta_2, \beta_3 > 0$, SP in the superlens–vacuum interface can be excited only when $k_x > \omega_0/c$, corresponding to the condition for the emission in part of the upper half-space: $90° < \theta < 180° - \theta_c$. Therefore, we can conclude that evanescent field components of the dipole field excite SPs in the superlens–vacuum interface, which are then converted into propagating waves in the prism.

5. FLUORESCENCE ENHANCEMENT

In order to examine the effectiveness of the proposed configuration to enhance fluorescence, fluorescence enhancement factors are calculated in this section by use of the equations

$$h_{\text{fluo}} = h_{\text{ex}} h_q,$$

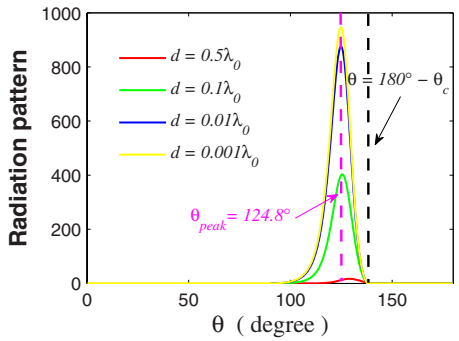

Fig. 7. (Color online) Radiation pattern. θ denotes the separation angle of the radiation direction with respect to the z axis.

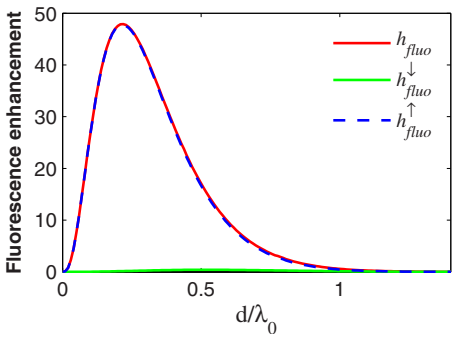

Fig. 8. (Color online) Fluorescence enhancement versus the position of the dipole. The peak position of the upper solid curve is (0.22, 47.90).

$$h_{\text{fluo}}^{\uparrow} = h_{\text{ex}} h_q^{\uparrow},$$

$$h_{\text{fluo}}^{\downarrow} = h_{\text{ex}} h_q^{\downarrow}, \tag{11}$$

where h_{fluo} is the total fluorescence enhancement factor, and $h_{\text{fluo}}^{\uparrow}$ and $h_{\text{fluo}}^{\downarrow}$ are two apparent fluorescence enhancement factors, corresponding to the radiation in the upper and the lower half-space, respectively. The calculated results are shown in Fig. 8. Fluorescence is quenched because of absorption by the superlens when d is very small. At a proper distance, fluorescence can be enhanced about 50 times. Our calculation also reveals that further reduction of $\text{Im}[\varepsilon_2(\omega_0)]$ and $\text{Im}[\mu_2(\omega_0)]$ will lead to even higher fluorescence enhancement factors. (The results are not shown here.) Another important feature that should be noted is that the radiation is confined to a small angular range (see Fig. 7), so that the fluorescence detection efficiency can be improved significantly. Therefore, the proposed configuration is proved to be highly effective in fluorescence detection.

6. CONCLUSION

In conclusion, we have analyzed theoretically the effectiveness of a new configuration composed of a prism and a superlens to enhance and detect fluorescence. Owing to the specific values of permittivity and permeability of the superlens, SP can be generated in the superlens–vacuum interface when a plane wave is incident on the superlens through the prism. This SP mode results in the excitation enhancement of the fluorescent dipole. In the fluorescent relaxation process, enhancement of quantum efficiency is calculated. Also, a surface polariton-coupled emission algorithm is formulated by comparing the calculated results in the relaxation process with those in the excitation process. Finally, fluorescence enhancement is obtained as the product of excitation enhancement and the enhancement of quantum efficiency. A large florescence enhancement (see Fig. 8) and the directional emission phenomenon (see Fig. 7) reveal the great potential of this configuration to be used in efficient fluorescence detection. The experimental challenge now is the fabrication of the superlens with small losses in the fluorescence excitation frequency, which should be the focus of further studies.

ACKNOWLEDGMENTS

We thank Shuang Zhang for inspiring discussions. This work was supported by the NSFC with grant 90923035, the 973 Program of China under grant 2006CB302904, and the "100 Projects" of Creative Research for Undergraduates of Nankai University under project BX6-293.

REFERENCES

1. R. W. Gruhlke, W. R. Holland, and D. G. Hall, "Surface-plasmon cross coupling in molecular fluorescence near a corrugated thin film," Phys. Rev. Lett. **56** 2838–2841 (1986).
2. H. Knobloch, H. Brunner, A. Leitner, F. Aussenegg, and W. J. Knoll, "Probing the evanescent field of propagating plasmon surface polaritons by fluorescence and Raman spectroscopies," J. Chem. Phys. **98**, 10093–10095 (1993).
3. J. Enderlein, "A theoretical investigation of single molecule fluorescence detection on thin metallic layers," Biophys. J. **78**, 2151–2158 (2000).
4. K. Vasilev, W. Knoll, and M. Kreiter, "Fluorescence intensities of chromophores in front of a thin metal film," J. Chem. Phys. **120**, 3439–3445 (2004).
5. J. R. Lakowicz, "Radiative decay engineering 3. Surface plasmon-coupled directional emission," Anal. Biochem. **324**, 153–169 (2004).
6. F. D. Stefani, K. Vasilev, N. Bocchio, N. Stoyanova, and M. Kreiter, "Surface-plasmon-mediated single-molecule fluorescence through a thin metallic film," Phys. Rev. Lett. **94**, 023005 (2005).
7. Y. J. Hung, I. I. Smolyaninov, C. C. Davis, and H. C. Wu, "Fluorescence enhancement by surface gratings," Opt. Express **14**, 10825–10830 (2006).
8. J. Gómez Rivas, G. Vecchi, and V. Giannini, "Surface plasmon-polariton mediated enhancement of the emission of dye molecules on metallic gratings," New J. Phys. **10**, 105007 (2008).
9. V. G. Veselago, "The electrodynamics of substances with simultaneously negative values of ε and μ," Sov. Phys. Usp. **10**, 509–514 (1968).
10. D. R. Smith, W. J. Padilla, D. C. Vier, S. C. Nemat-Nasser, and S. Schultz, "Composite medium with simultaneously negative permeability and permittivity," Phys. Rev. Lett. **84**, 4184–4187 (2000).
11. J. B. Pendry, "Negative refraction makes a perfect lens," Phys. Rev. Lett. **85**, 3966–3969 (2000).
12. R. Ruppin, "Surface polaritons of a left-handed medium," Phys. Lett. A **277**, 61–64 (2000).
13. R. Ruppin, "Surface polaritons of a left-handed material slab," J. Phys.: Condens. Matter **13**, 1811–1819 (2001).
14. I. V. Shadrivov, A. A. Sukhorukov, and Y. S. Kivshar, "Guided modes in negative-refractive-index waveguides," Phys. Rev. E **67**, 057602 (2003).
15. K. Park, B. J. Lee, C. Fu, and Z. M. Zhang, "Study of the surface and bulk polaritons with a negative index metamaterial," J. Opt. Soc. Am. B **22**, 1016–1023 (2005).
16. J. Kastel and M. Fleischhauer, "Suppression of spontaneous emission and superradiance over macroscopic distances in media with negative refraction," Phys. Rev. A **71**, 011804(R) (2005).
17. J. P. Xu, Y. P. Yang, H. Chen, and S. Y. Zhu, "Spontaneous decay process of a two-level atom embedded in a one-dimensional structure containing left-handed material," Phys. Rev. A **76**, 063813 (2007).
18. L. S. Froufe-Pérez and R. Carminati, "Controlling the fluorescence lifetime of a single emitter on the nanoscale using a plasmonic superlens," Phys. Rev. B **78**, 125403 (2008).
19. M. Born and E. Wolf, *Principles of Optics*, 7th ed. (Cambridge Univ. Press, 1999).
20. L. Novotny and B. Hecht, *Principles of Nano-Optics* (Cambridge Univ. Press, 2006).